

All-optical switching of spins in ferromagnetic Co/Pt with a single dual pulse

Kihiro T. Yamada^{1,2*}, Alexey V. Kimel^{1,*}, Sergiu Ruta³, Roy Chantrell³,

Kiran Horabail Prabhakara¹, Tian Li⁴, Fuyuki Ando⁴, Sergey Semin¹,

Teruo Ono^{4,5}, Andrei Kirilyuk^{1,6}, and Theo Rasing¹

¹*Institute for Molecules and Materials, Radboud University, Nijmegen 6525 AJ, The Netherlands*

²*Department of Physics, Tokyo Institute of Technology, Tokyo 152-8551, Japan.*

³*Department of Physics, University of York, Heslington, York YO10 5DD, United Kingdom.*

⁴*Institute for Chemical Research, Kyoto University, Uji, Kyoto 611-0011, Japan.*

⁵*Center for Spintronics Research Network (CSRN), Graduate School of Engineering Science,
Osaka University, Toyonaka, Osaka 560-8531, Japan.*

⁶*FELIX Laboratory, Radboud University, Toernooiveld 7c, Nijmegen 6525 ED, The Netherlands.*

*email: yamada@phys.titech.ac.jp; aleksei.kimel@ru.nl

All-optical magnetic recording can achieve breakthroughs in information technologies by merging the advantages of photonics, facilitating the fastest and nearly non-dissipative information transfer, with the unique properties of magnets allowing non-volatile storage of information¹⁻⁵. However, all-optical magnetic recording in a ferromagnetic metal by circularly polarized light requires many pulses for full switching⁶⁻¹³. Here, we demonstrate efficient all-optical helicity dependent magnetic recording using a single pair of femto/pico-second laser pulses. Changing the time separation between the pulses and the helicity of the second, picosecond, pulse, we succeeded to switch the magnetization of at least 80% of the irradiated area. Using both experimental and computational approaches, we show that the most efficient switching is realized when the first, femtosecond pulse of the pair brings the ferromagnet into a strongly nonequilibrium, nearly demagnetized state, while the second, circularly polarized picosecond pulse deterministically controls picosecond relaxation from this state by helicity dependent laser absorption.

Light, laser technologies, and photonics play decisive roles in the development of telecommunication as well as facilitating the fastest and most energy-efficient transfer of data around the Globe. Similarly, magnetism offers a natural, reliable, nonvolatile, and therefore energy efficient way to store digital data. Interfacing magnetism and photonics can be seen as the next challenge for our digital society¹, which can lead to breakthroughs in information technologies as well as facilitate new applications of computers², by merging the fast and energy-efficient nature of optical communication with the non-volatility of magnets¹⁻⁵. While state-of-the-art magnetic data storage employs ferromagnets as a storage medium, practically all the experiments on ultrafast all-optical magnetic recording with a single femtosecond laser pulse have been realized on ferrimagnetic materials³⁻⁵. This is why the discovery of all-optical helicity dependent switching (AO-HDS) of magnetic domains in ferromagnetic Co/Pt multilayers⁶⁻¹² and FePt granular media¹³ greatly boosted the interest in the field and initiated intense discussions about the mechanism of the phenomenon. However, in all the experiments, the switching took at least tens of laser pulses⁶⁻¹², lasted at least milliseconds, and appeared to proceed via two stages: helicity independent demagnetization and helicity dependent domain wall motion⁷.

The goal of our study was to find the shortest possible combination of pulses that allows switching the magnetization of ferromagnetic materials in a helicity dependent and deterministic way. The earlier demonstration of the two-step mechanism⁷ inspired us to propose a dual pulse excitation in which each pulse of a pair of pulses is optimized for either the helicity independent demagnetization or the helicity dependent domain wall motion. The dual-pulse-excitation concept is shown in Fig. 1a. The studied Pt/Co/Pt trilayer with perpendicular magnetic anisotropy is excited by two laser pulses. The pair consists of a femtosecond linearly polarized (π) laser pulse, meant to demagnetize the sample and a picosecond circularly polarized (σ) laser pulse, meant to steer the

magnetization to its final state in a helicity dependent way, but without causing further demagnetization. Varying the time separation (Δt) between the pulses, we searched for the optimal combination for the switching.

After finding such a combination, we used magneto-optical measurements with sub-picosecond resolution and revealed sub-10 ps dynamics triggered by the pulse pair. It is shown that the first fs π pulse of the pair demagnetizes the ferromagnet and results in a drop of the average magnetization down to 20 %. If the picosecond σ laser pulse arrives not later than 5 ps after the first pulse, the helicity dependent absorption of the picosecond σ laser pulse controls the relaxation from the demagnetized state and eventually results in magnetization reversal.

We prepared a Pt/Co/Pt stack, which is a typical candidate for spintronic devices¹⁴ as well as for all-optical helicity dependent switching⁶⁻¹². To characterize the switching in the studied structure, we measured first the switching with only circularly polarized pulses. Figure 1b shows magneto-optical images taken after the Pt/Co/Pt film was excited with a sequence of 4.5-ps right(σ^+)- or left(σ^-)-handed circularly polarized light pulses. The images were taken long after the excitation when the magnetization had already reached a stable state. The interval between the pulses was set to be at least 2 seconds. The measurements confirm that ps σ pulses are more favorable for the AO-HDS than fs σ pulses (See ref. 9 and Supplementary Fig. 2). The interval between the pulses was set to be at least 2 seconds. In agreement with previous experiments⁹, the switching proceeds via a partial demagnetization at the spot center, nucleation of switched domains, and helicity dependent domain wall motion. The main driving force of the motion originates from a temperature difference between M^\uparrow and M^\downarrow domains created via optical magnetic circular dichroism (MCD) (See Supplementary Figs. 4 and 5). In order to fully switch the magnetization in the area with a diameter of 15- μm , the experiments required 120-140 pulses.

Similar experiments with a pair of pulses shows that the duration of the laser excitation required for the switching can be reduced substantially. Figure 1c shows the results of an experiment, in which the same Pt/Co/Pt stack was excited with one 90-fs π and one 4.5-ps σ pulses, separated by $\Delta t = 5.0$ ps. It is seen that a single pair of these pulses can switch a substantial (>80%) part of the same 15- μm area in a helicity dependent and deterministic way. In the case of excitation without π pulses, i.e. with σ pulses only, a similar result would require about 100 excitation events. The polarization of the 90-fs π pulse does not determine the switching (See Supplementary Fig. 8).

To find the optimal combination of the pulses for the switching, we first performed measurements as a function of Δt of the pair. The averaged net magnetization $\langle M \rangle$ after illumination with a pulse pair as a function of Δt is shown in Fig. 2b. $\langle M \rangle$ was determined by averaging the intensities of all the pixels in the 15- μm -area and normalized to the average intensity of the image for a uniformly magnetized sample. Figure 2c shows the helicity dependent switching efficiency, which is defined as $[\langle M \rangle(M^\uparrow, \sigma^+) - \langle M \rangle(M^\uparrow, \sigma^-) + \langle M \rangle(M^\downarrow, \sigma^+) - \langle M \rangle(M^\downarrow, \sigma^-)] / 4$, as a function of Δt . Here, (M^\uparrow, σ^+) means that the magnetic state was originally saturated in the up direction and the ps pulse was right-handed circularly polarized, etc. It is seen that the optimal switching is obtained when the ps σ pulse arrives around 5.0 ps after the fs π pulse. Longer separation reduces the switching efficiency dramatically. No switching and only demagnetization is observed if the fs π pulse arrives after the ps σ pulse. Note that, within 5 ps after the excitation with a femtosecond pulse, no domains have been formed yet and the medium must still be in strong non-equilibrium, a nearly demagnetized state. The delay of 5 ps is within the ball-park of the characteristic times of the electron-phonon interaction in metals. Therefore, the experiments show that the circularly polarized pulse can deterministically steer the relaxation to one or another stable state in a helicity dependent way only if the electron gas is out of equilibrium with the lattice.

To reveal the ultrafast dynamics of the helicity dependent switching with the pulse pair, we performed stroboscopic experiments. We excited the sample with a sequence of the pairs and measured the magnetization dynamics integrated over the excited area with the help of the magneto-optical Faraday effect. To ensure that the magnetization relaxes back to the initial state before the next pair arrives, after every switching event with a single pair, we applied a small magnetic field of 3.3 mT. Such a field corresponds to a spin precession with a period of ~ 11 ns. In this way, the field can restore the initial magnetization within 2 ms (separation between the pairs in the experiment). Figure 3a reveals sub-10 ps dynamics triggered by the pair of π and σ pulses, measured for two helicities of the σ pulse. It is seen that the fs π pulse brings the medium into a nearly demagnetized state. This excitation is followed by a ps relaxation which is affected by the ps σ pulse in a helicity dependent way. The helicity dependence of the dynamics disappears upon increasing Δt between the pulses from 2.5 ps to 7.5 ps (see Fig 3b). Particularly, in the measurements with $\Delta t = 7.5$ ps, it is seen that after excitation with the first fs laser pulse the magnetization first drops down to 20% and later partially recovers on a time scale of 5 ps. In the conventional three-temperature model of ultrafast demagnetization, this recovery time is assigned to the characteristic time of electron-phonon interaction.

Interestingly, a much smaller helicity dependence is observed in stroboscopic experiments with just ps σ pulses, when the π -pulses are blocked (see Supplementary Fig. 9). Therefore, our experiments reveal that the largest sensitivity of the magnetization dynamics in Co/Pt to the helicity of light is achieved when the electrons in the material are hot and thus in a highly non-equilibrium state. Despite the clear switching long after the action of the pair (Fig. 1c) and the observed helicity dependent dynamics within the action of the σ pulse (Fig. 3), we do not see a substantial difference in magnetization after the action of the ps σ pulse. This means that the

differences that later evolve into a switched domain are too small to be seen in our optical experiments. Estimating the signal-to-noise ratio in the stroboscopic experiment shown in Fig. 3a at the level of 100 allows obtaining the maximum possible area of a feature, which cannot be resolved in our experiment, at the level of $\frac{15\mu m \times 15\mu m}{100} \approx 2\mu m^2$. It is proposed that sub-20 ps relaxation leads to the formation of sub-micron nuclei with a reversed magnetization. Experimental observation of these nuclei can be seen as the next challenge in ultrafast all-optical switching of magnetism.

To reveal the spatial aspects of the ultrafast magnetization dynamics (on the order of 1-2 nm), we have developed an atomistic scale model (see Methods) of the switching process. It describes the production of randomly oriented nanometer-scale nuclei after ultrafast demagnetization due to the first π pulse and the differential (helicity dependent) heating of the nuclei by the second σ pulse. First, the average magnetization of the overall system is evaluated as a function of laser power and Δt between the two pulses (a 90-fs π pulse, followed by a 4.5 ps σ pulse). Deterministic switching is observed for a fluence of 1.25 mJ/cm² and Δt between 0.5 ps and 3.5 ps (see Fig. 4a). The averaged magnetization m_z and electron temperatures T_e as a function of delay time t is shown in Fig. 4b for $\Delta t = 2.5$ ps and 5.0 ps, respectively. Also, the m_z and temperature maps are shown in Figs. 4c-j. The first π pulse elevates T_e and demagnetizes the system (Fig. 4b). This demagnetization destroys any macroscopic domain configurations to create small, non-equilibrium, and localized magnetic textures¹⁵. (Figs. 4c and 4g). These small spin textures are not stable, but they can grow/evolve to larger stable domain structures by a small asymmetry in the local temperature in the spin system produced by the helicity dependent absorption of the second σ laser pulse originating from magnetic circular dichroism. If this temperature difference exists immediately after the demagnetization state at $t \sim 1$ ps (Fig. 4e), the hotter M^\uparrow nuclei become

unstable and shrink in size and the cooler M^\downarrow nuclei grow to form the dominant region in the system (Fig. 4d). This process is present in the simulations for Δt up to 3.5 ps. However, when the second pulse is applied at larger Δt , the spin textures have become too large to change by a temperature difference of about 10-20K (see Fig. 4h and 4j). The difference in the temperature between M^\uparrow and M^\downarrow textures must therefore be formed while the textures are small. Hence, both the experimental findings and the simulations emphasize the importance of having the second σ pulse when the magnetic medium is still in a strongly non-equilibrium spin state created by the first short π pulse.

To summarize, we found the optimal and shortest combination of laser pulses allowing to switch the magnetization of Co/Pt in a helicity dependent and deterministic way in around 5 ps. The switching is achieved for excitation with a pair of 90 fs linearly polarized and 4.5 ps circularly polarized laser pulses separated by no more than 5 ps. In this case, the femtosecond laser pulse brings the medium into a strongly non-equilibrium, nearly demagnetized state. The excitation is followed by a picosecond relaxation on a time scale of 5.0 ps. The second picosecond circularly polarized pulse affects the relaxation in a helicity dependent way, which strongly depends on the time separation between the pulses. Although atomistic simulations are intrinsically unable to reproduce the magnetization dynamics of micron size objects, the modeling, similar to the experiment, emphasizes that for a successful switching the second σ pulse must find Co/Pt in strong nonequilibrium. Moreover, the model calculations show that the reversal proceeds via nm-scale nuclei existing in the strongly non-equilibrium state prepared by the first short π pulse. Reversal via such nuclei is distinct from the switching of stable domains as in previous experiments^{7,9} which relies on domain expansion via the relatively slow mechanism of domain wall motion. Manipulation of the magnetization on this time- and length- scale opens the possibility of new approaches to ultrafast spin dynamics and shows considerable promise for the

switching of nanoscale ferromagnetic materials for future information storage. Our results reveal that both ultrafast magnetization dynamics and the efficiency of the switching are most sensitive to the helicity of the circularly polarized pulse when the latter finds the sample in the state with a hot electron gas.

References

1. Kimel, A. V. & Li, M. Writing magnetic memory with ultrashort light pulses. *Nat. Rev. Mater.* **4**, 189-200 (2019).
2. Manipatruni, S., Nikonov, D. E. & Young, I. A. Beyond CMOS computing with spin and polarization. *Nat. Phys.* **14**, 338-343 (2018).
3. Stanciu, C. D., Hansteen, F., Kimel, A. V., Kirilyuk, A., Tsukamoto, A., Itoh, A. & Rasing, Th. All-optical magnetic recording with circularly polarized light. *Phys. Rev. Lett.* **99**, 047601 (2007).
4. Ostler, T. A., Barker, J., Evans, R. F. L., Chantrell, R. W., Atxitia, U., Chubykalo-Fesenko, O., Moussaoui, S. El, Guyader, L. Le, Mengotti, E., Heyderman, L. J., Nolting, F., Tsukamoto, A., Itoh, A., Afanasiev, D., Ivanov, B. A., Kalashnikova, A. M., Vahaplar, K., Mentink, J., Kirilyuk, A., Rasing, Th. & Kimel, A. V., Ultrafast heating as a sufficient stimulus for magnetization reversal in a ferrimagnet. *Nat. Commun.* **3**, 666 (2012).
5. Khorsand, A. R., Savoini, M., Kirilyuk, A., Kimel, A. V., Tsukamoto, A., Itoh, A. & Rasing, Th. Role of magnetic circular dichroism in all-optical magnetic recording. *Phys. Rev. Lett.* **108**, 127205 (2012).

6. Lambert, C.-H., Mangin, S., Varaprasad, B. S. D. Ch. S., Takahashi, Y. K., Hehn, M., Cinchetti, M., Malinowski, G., Hono, K., Fainman, Y., Aeschlimann, M. & Fullerton, E. E. All-optical control of ferromagnetic thin films and nanostructures. *Science* **345**, 1337-1340 (2014).
7. Hadri, M. S. El, Pirro, P., Lambert, C.-H., Petit-Watelot, C.-H., Quessab, Y., Hehn, M., Montaigne, F., Malinowski, G. & Mangin, S. Two types of all-optical magnetization switching mechanisms using femtosecond laser pulses. *Phys. Rev. B* **94**, 064412 (2016).
8. Hadri, M. S. El, Hehn, M., Pirro, P., Lambert, C.-H., Malinowski, G., Fullerton, E. E. & Mangin, S. Domain size criterion for the observation of all-optical helicity-dependent switching in magnetic thin films. Two types of all-optical magnetization switching mechanisms using femtosecond laser pulses. *Phys. Rev. B* **94**, 064419 (2016).
9. Medapalli, R., Afanasiev, D., Kim, D. K., Quessab, Y., Manna, S., Montoya, S. A., Kirilyuk, A., Rasing, Th., Kimel, A. V. & Fullerton, E. E. Multiscale dynamics of helicity-dependent all-optical magnetization reversal in ferromagnetic Co/Pt multilayers. *Phys. Rev. B* **96**, 224421 (2017).
10. Quessab, Y., Medapalli, R., El Hadri, M. S., Hehn, M., Malinowski, G., Fullerton, E. E. & Mangin, S. Helicity-dependent all-optical domain wall motion in ferromagnetic thin. *Phys. Rev. B* **97**, 054419 (2018).
11. Parlak, U., Adam, R., Bürgler, D. E., Gang, S. & Schneider, C. M. Optically induced magnetization reversal in $[\text{Co/Pt}]_N$ multilayers: Role of domain wall dynamics. *Phys. Rev. B* **98**, 214443 (2018).

12. Kichin, G., Hehn, M., Gorchon, J., Malinowski, G., Hohlfeld, J. & Mangin, S. From Multiple- to Single-Pulse All-Optical Helicity-Dependent Switching in Ferromagnetic Co / Pt Multilayers. *Phys. Rev. Applied* **12**, 024019 (2019).
13. John, R., Berritta, M., Hinzke, D., Müller, C., Santos, T., Ulrichs, H., Nieves, P., Walowski, J., Mondal, R., Chubykalo-Fesenko, O., McCord, J., Oppeneer, P. M., Nowak, U. & Münzenberg, M. Magnetisation switching of FePt nanoparticle recording medium by femtosecond laser pulses. *Sci. Rep.* **7**, 4114 (2017).
14. Brataas, A., Kent, A. D. & Ohno, H. Current-induced torques in magnetic materials. *Nat. Mater.* **11**, 372-381 (2012).
15. Iacocca, E., Liu, T-M., Reid, A. H., Fu, Z., Ruta, S., Granitzka, P. W., Jal, E., Bonetti, S., Gray, A. X., Graves, C. E., Kukreja, R., Chen, Z., Higley, D. J., Chase, T., Guyader, L. Le, Hirsch, K., Ohldag, H., Schlotter, W. F., Dakovski, G. L., Coslovich, G., Hoffmann, M. C., Carron, S., Tsukamoto, A., Savoini, M., Kirilyuk, A., Kimel, A. V., Rasing, Th., Stöhr, J., Evans, R. F. L., Ostler, T., Chantrell, R. W., Hoefer, M. A., Silva, T. J. & Dürr, H. A. Spin-current-mediated rapid magnon localisation and coalescence after ultrafast optical pumping of ferrimagnetic alloys. *Nat. Commun.* **10**, 1756 (2019).

Methods

Sample preparations. The multilayer of Ta (4 nm)/Pt (3.0 nm)/Co (0.8 nm)/Pt (3.0 nm)/MgO (2.0 nm)/Ta (1.0 nm) was sputtered on a synthetic quartz glass substrate. DC and RF sources were used for depositing Ta, Pt, and Co, and MgO, respectively. The MgO/Ta capping layer prevents the magnetic layer from oxidization. The multilayer exhibits a perpendicular easy axis of magnetization. The effective magnetic anisotropy field and constant are 1.16 T and 9.4×10^5 J/m³,

respectively, with a typical saturation magnetization of 1.6×10^6 A/m. Using these magnetic parameters, the exchange stiffness constant was estimated to be 9.8×10^{-12} J/m from the equilibrium domain width ($14.5 \mu\text{m}$)¹⁶.

Magneto-optical imaging. For optical excitation, we used a Ti: sapphire amplified laser system (Solstice Ace, Spectra-Physics) of which the central wavelength and repetition rate were 800 nm and 1 kHz, respectively. The amplifier system contains two compressors which allowed independent control of the pulse width for the two pump beams. The laser amplifier was used in external trigger mode, in which, with the help of a delay generator (DG645, Stanford Research) we can control the number of pulses reaching the sample. Magneto-optical Faraday imaging with a white light source as probe was employed for detection, see Supplementary Fig. 1a. The duration of the first linearly polarized pump pulse was about 90 fs while the second, circularly polarized pump pulse, was 4.5 ps long and arrived after an adjustable pulse interval, Δt . The laser pulses had a Gaussian intensity distribution and both were incident at an angle of 15 deg. from the sample normal. The focused beam sizes ($1/e^2$ radius) of the π and σ pump pulses were calculated with the Liu method^{5,17} to be $35.5 \pm 0.7 \mu\text{m}$ and $42.9 \pm 0.4 \mu\text{m}$, respectively. The laser fluence was calculated using the $1/e^2$ radius, the repetition rate (1 kHz), and the average power measured with a power meter. The pump intensity was controlled using a combination of a half-wave plate and a Gran-Taylor prism. To achieve precise intensity control of the circularly-polarized pump, the half-wave plate was mounted on a motorized stage. A quarter-wave plate was placed after the Gran-Taylor prism to convert the linearly polarized beam to a circularly polarized one for the second pump. The probe light from the white light source was linearly polarized by a sheet polarizer. It was then collimated and incident on the sample surface using a combination of lenses. The

transmitted light from the sample was collected by an objective with a magnification of 20 \times . An analyzer, with the polarization axis orthogonal to the polarization of the incident probe light, was placed before a charge-coupled device (CCD) camera.

Time-resolved magneto-optical measurements. For the pump-probe measurements, the laser amplifier was operated in the internal trigger mode at 1 kHz. See Supplementary Fig. 1b for the schematic. An optical parametric amplifier was used to tune the wavelength of the output from the internal compressor to 1000 nm. Moreover, the output from the optical parametric amplifier was separated into two beams. One was used as the first π pump pulse after the wavelength was converted to 500 nm by a Beta barium borate (BBO) crystal. We put a delay line on the other beam, which was used as the probe beam. We used the output from the external compressor for the σ pulse as done in the static measurements. The repetition rates of the two pump pulses were brought down to 500 Hz by a mechanical chopper. After the intensity of the probe beam was weakened by a combination of a half-wave plate and a Gran-Taylor prism, the probe beam was incident onto the film surface. The transmitted light collected by the objective went through a long pass filter into a balanced detector to measure the Faraday rotation. While varying the delay line, we measured the perpendicular magnetization component through the Faraday effect at an arbitrary time before and after the pump pulses arrived at the sample. During the pump-probe measurements, we applied a magnetic field of 3.3 mT along the normal to the sample to initiate the magnetic state. The field was generated by two permanent magnets on either side of the sample. The $1/e^2$ radii were $31.6 \pm 0.7 \mu\text{m}$, $29.7 \pm 0.9 \mu\text{m}$, and $62.7 \pm 1.4 \mu\text{m}$ for the probe, the short π polarized, and the long σ beams, respectively. We fixed the fluence of the probe beam at 0.32 mJ/cm^2 , which was much smaller than those of the π and σ pump beams (2.31 mJ/cm^2 and 2.50 mJ/cm^2 , respectively).

Atomistic spin dynamics simulations. For the numerical investigation of spin dynamics under the pulse laser excitation, we developed an atomistic spin dynamics (ASD) model of Co thin films.

The energy of the system is described by the spin Hamiltonian:

$$\mathcal{H} = - \sum_{i < j} J_{i,j} S_i \cdot S_j - \sum_i k_u (S_i^z)^2,$$

where the spin S_i is a unit vector describing the local spin direction. It is normalized to the local atomic spin magnetic moment (μ_s). We use $\mu_{\text{Co}} = 1.61 \mu_B$ and nearest neighbor Co-Co exchange of $J = 4.8 \times 10^{-21}$ J.

The ASD allows atomistic level resolution of spin dynamics, which is important in understanding small spin textures forming immediately after the laser excitation. The compromise is that the simulated systems are relatively small. In this case, we consider a 50 nm×50 nm× 10nm thin film. To be able to capture multiple domain structures, the anisotropy was enhanced such that the smallest stable domain to be around 6 nm.

The magnetic anisotropy, k_u , was taken 5.85×10^{-23} J, one order of magnitude larger than reported in the literature¹⁸. The VAMPIRE software package¹⁹ developed by the group of R. Chantrell at University of York was used to compute the system dynamics based on the Landau-Lifshitz-Gilbert (LLG) equation:

$$\frac{\partial S_i}{\partial t} = - \frac{\gamma}{(1 + \alpha^2)} [S_i \times B_{\text{eff}}^i + \alpha_i S_i \times (S_i \times B_{\text{eff}}^i)],$$

where γ is the gyromagnetic ratio and α is the Gilbert damping factor. The on-site effective field can be computed as the summation of the local field derived from the spin Hamiltonian with a random field to model the heat bath:

$$B_{\text{eff}}^i = - \frac{\partial \mathcal{H}}{\partial S_i} + \zeta_i,$$

where ζ_i is a stochastic thermal field due to the interaction of the conduction electrons with the local spins. The stochastic thermal field is assumed to have Gaussian statistics and satisfies:

$$\langle \zeta_{i,a}(t) \zeta_{j,b}(t') \rangle = \delta_{ij} \delta_{ab} (t - t') 2\alpha_i k_B T \mu_i / \gamma_i$$

$$\langle \zeta_{i,a}(t) \rangle = 0,$$

where k_B is the Boltzmann constant and T is the temperature. We incorporate the rapid change in thermal energy of a system under the influence of a femtosecond laser pulse. The spin system is coupled to the electron temperature, T_e , which is calculated using the two-temperature model²⁰:

$$T_e C_e \frac{dT_e}{dt} = -G_{el}(T_l - T_e) + P(t),$$

$$C_l \frac{dT_l}{dt} = -G_{el}(T_e - T_l),$$

where the $C_e = 700 \text{ Jm}^{-3} \text{ K}^{-1}$, $C_l = 3.0 \times 10^6 \text{ Jm}^{-3} \text{ K}^{-1}$, and $G_{el} = 1.7 \times 10^{17} \text{ Wm}^{-3} \text{ K}^{-1}$ were used. $P(t)$ models the temperature from the laser pulse into the electronic system. Here, we consider a combination of two pulses: first linear polarized pulse and second circularly polarized pulse. We model this by considering $P(t) = P_1(t) + [1 - f_{\text{MCD}}(s_z)]P_2(t)$, where $f_{\text{MCD}}(s_z)$ is assumed in first approximation linear function between 0 for $s_z = 1$ and the MCD value for $s_z = -1$.

References

16. Sukstanskii, A. L. & K. I. Primak, K. I., Domain structure in an ultrathin ferromagnetic film. *J. Magn. Magn. Mater.* **169**, 31 (1997).
17. Liu, J. M. Simple technique for measurements of pulsed Gaussian-beam spot sizes. *Opt. Lett.* **7**, 196-198 (1982).

18. Moreno, R., Evans, R. F. L., Khmelevskiy, S., Muñoz, M. C., Chantrell, R. W. & Chubykalo-Fesenko, O. Temperature-dependent exchange stiffness and domain wall width in Co. *Phys. Rev. B* **94**, 104433 (2016).
19. Evans, R. F. L., Fan, W. J., Chureemart, P., Ostler, T. A., Ellis, M. O. A. & Chantrell, R. W. Atomistic spin model simulations of magnetic nanomaterials. *J. Phys.: Condens. Matter* **26**, 103202 (2014).
20. Jiang, L. & Tsai, H.-L. Improved two-temperature model and its application in ultrashort laser heating of metal films. *J. Heat Transfer*. **127**, 1167–1173 (2005).

Data availability

The data that support the findings of this study are available from the corresponding author upon reasonable request.

Acknowledgement

We thank T. Toonen and C. Berkhout for the continuous technical supports, J. Mentink and T. Satoh for the fruitful discussions, and T. Taniguchi for the valuable comments on sample fabrication. We are grateful for computational support from the University of York High-Performance Computing service, VIKING and the Research Computing team. This work was partly supported by the European Research Council Grant Agreement No.856538 (3D-MAGiC), by the FOM programme Exciting Exchange, de Nederlandse Organisatie voor Wetenschappelijk Onderzoek (NWO), by the EU H2020 Program Grant Agreement No. 713481 (SPICE) and No.

737093 (FEMTOTERABYTE), by JSPS KAKENHI No. 15H05702, No. 20H00332, No. 20H05665, No. 17J07326, and No. 18J22219, and by the Collaborative Research Program of the Institute for Chemical Research, Kyoto University. The atomistic simulations were undertaken on the Viking cluster, which is a high-performance computing facility provided by the University of York.

Author contributions

K.T.Y., A.V.K., and T.R. conceived the experiments. K.T.Y., K.H.P., and S.S. designed and build the experimental set-up. K.T.Y. performed the measurements, and collected data. All the data were analyzed by K.T.Y. with the help of A.V. K and T.R. S.R. and R.W.C. performed the simulations. The samples were fabricated and provided by T.L., F.A., and T.O. K.T.Y., A.V.K., S.R. and T.R. wrote the manuscript. All authors discussed the results and commented on the manuscript. This project was coordinated by A.V.K. and T. R.

Competing interests

The authors declare no competing interests.

Additional information

Supplementary information is available for this paper at [URL inserted by publisher].

Correspondence and requests for materials should be addressed to K.T.Y. and A.V.K.

Reprints and permissions information is available at www.nature.com/reprints.

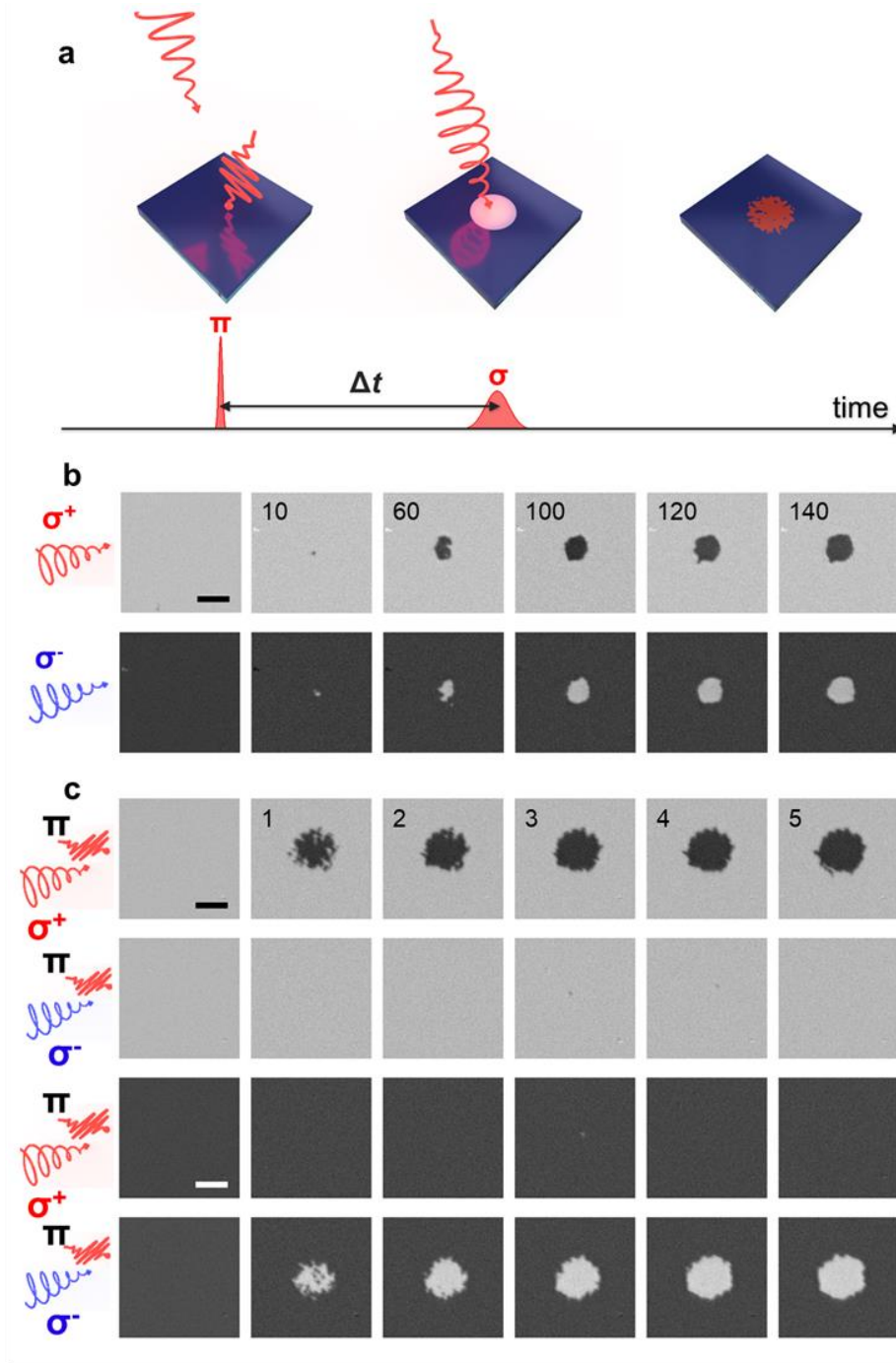


Fig 1 | Dual-pulse all-optical helicity dependent switching (AO-HDS). **a**, Principal concept of dual-pulse AO-HDS. **b**, AO-HDS by multiple right(σ^+) and left (σ^-) circularly polarized pulses. Here, the fluence of the 4.5-ps σ pulse was fixed at $F_\sigma = 4.87 \text{ mJ/cm}^2$. **c**, Dual-pulse AO-HDS for time separation Δt of 5.0 ps. Here, we used the fluence of $F_\pi = 2.32 \text{ mJ/cm}^2$ for the 90-fs π pulse and $F_\sigma = 2.37 \text{ mJ/cm}^2$. The number of pulse (pairs) is indicated on each magneto-optical image. The darker and brighter areas denote up(M^\uparrow)- and down(M^\downarrow)-magnetized states, respectively. The scale bars correspond to 20 μm .

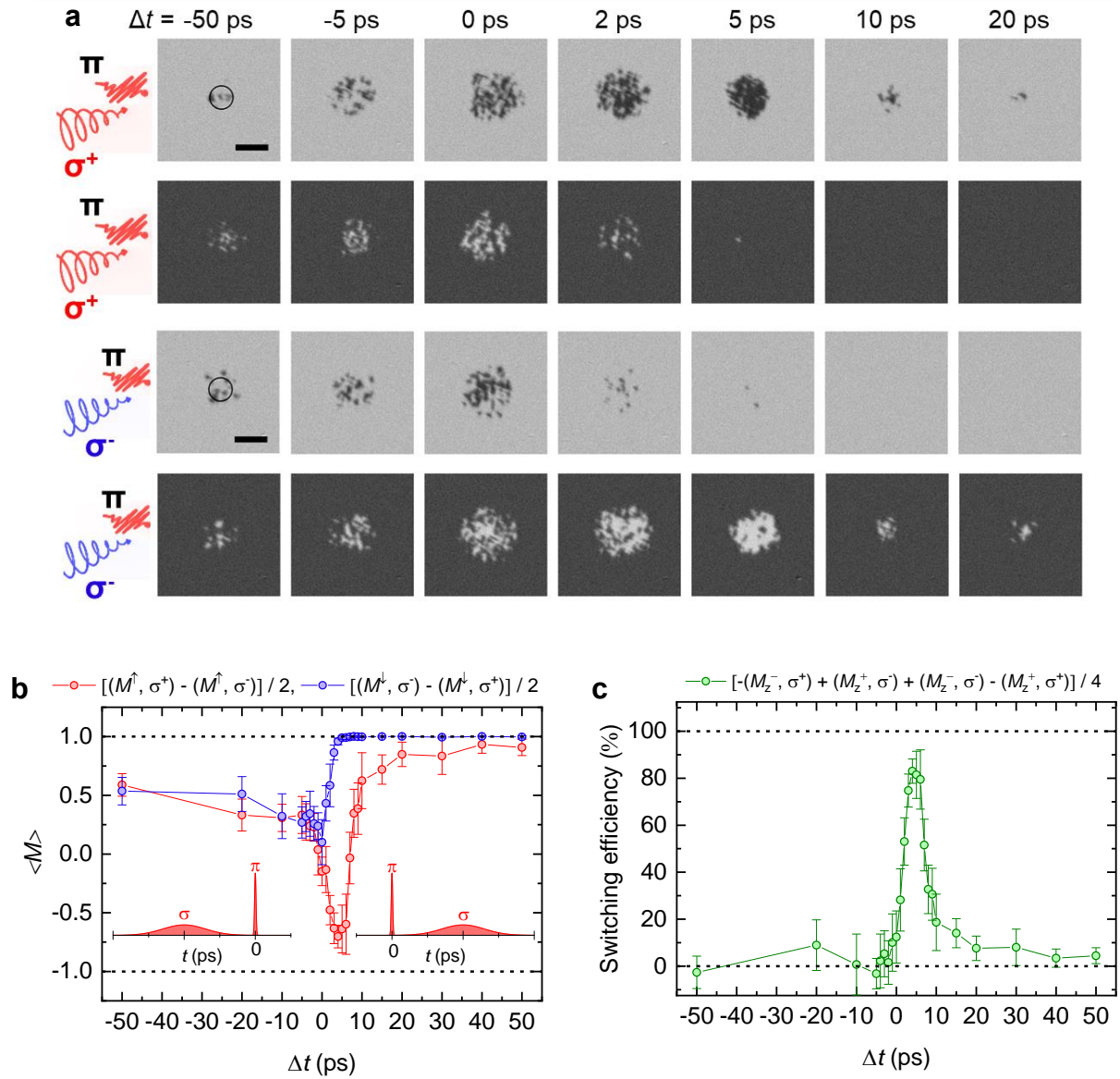


Fig 2 | The time-separation dependence of the AO-HDS. **a**, Magneto-optical images after the excitation of a pulse pair for various Δt . The laser parameters were the same as in Fig.1c. The scale bars correspond to $20 \mu\text{m}$. A $15\text{-}\mu\text{m}$ diameter area for integration is indicated by a solid-line circle. **b**, **c**, Average net magnetization $\langle M \rangle$ (**b**) and switching efficiency (**c**) after the illumination of a pulse pair as a function of Δt . We defined the switching efficiency as $[\langle M \rangle (M^\uparrow, \sigma^+) - \langle M \rangle (M^\uparrow, \sigma^-) + \langle M \rangle (M^\downarrow, \sigma^-) - \langle M \rangle (M^\downarrow, \sigma^+)] / 4$. Here, (M^\uparrow, σ^+) means that right circularly polarized pulse was given to the up-magnetized background. As shown in the insets of Fig. 2b, the positive (negative) Δt means that the long σ pulse reaches the sample later (earlier) than the short π pulse. The error bars were determined by repeating the same measurements five times.

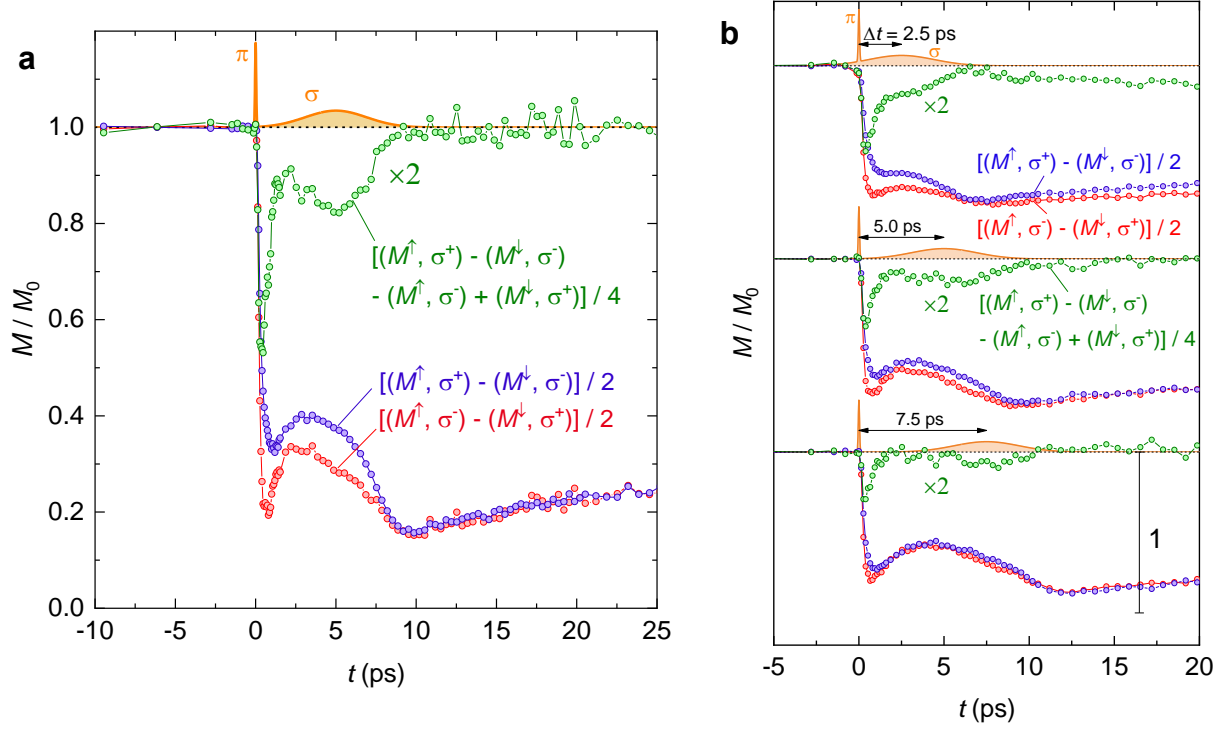


Fig. 3 | Time-resolved magneto-optical measurements. **a**, The normalized magnetization M / M_0 as a function of delay time t for $\Delta t = 5.0$ ps with the dual-pulse excitation. Here, we used $F_\pi = 2.31$ mJ/cm² and $F_\sigma = 2.50$ mJ/cm². A magnetic field of 3.3 mT was applied to ensure that the magnetization relaxes back to the initial state. **b**, The time evolution of M / M_0 and the difference for $\Delta t = 2.5$ ps, 5.0 ps, and 7.5 ps. The Gaussian time profiles of the 90-fs π pulse and 4.5-ps σ pulse are also shown in the plots, where the peak heights were arbitrarily tuned for simplicity.

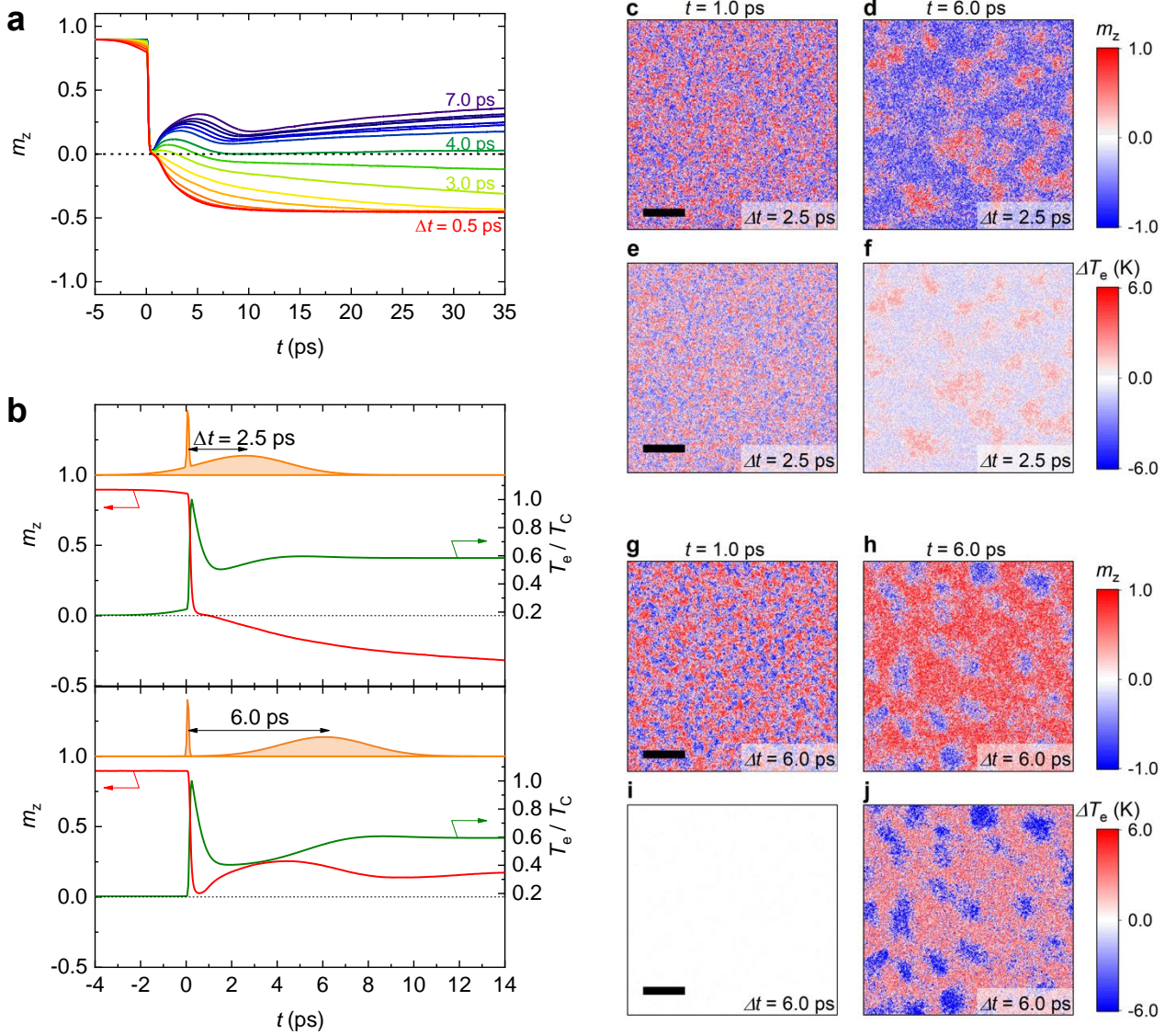


Fig 4 / The atomistic spin simulation of time-resolved magnetization dynamics in the first 35 ps after the pulse pair. a, The z component of magnetization m_z as a function of t for Δt in the range of 0.5 ps – 6.5 ps. **b,** The electron temperature T_e and m_z as a function of t for $\Delta t = 2.5$ ps and 6.0 ps. The value of T_e was normalized with the Curie temperature T_C for comparison. The laser pulse profiles are illustrated together. **c-j,** The m_z and temperature maps for $\Delta t = 2.5$ ps (**c-f**) and 6.0 ps (**g-j**). The temperature map represents the difference ΔT_e between the local temperature and the average T_e per site. The scale bars correspond to 10 nm. The maximum temperature difference between up- and down-magnetized nuclei was around (10-20K). The temperature difference lasts for about 10 ps.